Environmental Science and Pollution Research (2018) 25:20591–20605
https://doi.org/10.1007/s11356-018-2238-1

RESEARCH ARTICLE

Chemical characterization of $PM_{2.5}$ from a southern coastal city of China: applications of modeling and chemical tracers in demonstration of regional transport

Jiamao Zhou[1,2] · Steven Sai Hang Ho[1,3] · Junji Cao[1] · Zhuzi Zhao[1] · Shuyu Zhao[1] · Chongshu Zhu[1] · Qiyuan Wang[1] · Suixin Liu[1] · Ting Zhang[1] · Youzhi Zhao[4] · Ping Wang[4] · Xuexi Tie[1]

Received: 9 November 2017 / Accepted: 4 May 2018 / Published online: 11 May 2018

Abstract

An intensive sampling campaign of airborne fine particles ($PM_{2.5}$) was conducted at Sanya, a coastal city in Southern China, from January to February 2012. Chemical analyses and mass reconstruction were used identify potential pollution sources and investigate atmospheric reaction mechanisms. A thermodynamic model indicated that low ammonia and high relative humidity caused the aerosols be acidic and that drove heterogeneous reactions which led to the formation of secondary inorganic aerosol. Relationships among neutralization ratios, free acidity, and air-mass trajectories suggest that the atmosphere at Sanya was impacted by both local and regional emissions. Three major transport pathways were identified, and flow from the northeast (from South China) typically brought the most polluted air to Sanya. A case study confirmed strong impact from South China (e.g., Pearl River Delta region) (contributed 76.8% to EC, and then this result can be extended to primary pollutants) when the northeast winds were dominant. The Weather Research Forecasting Black carbon model and trace organic markers were used to apportion local pollution versus regional contributions. Results of the study offer new insights into the atmospheric conditions and air pollution at this coastal city.

Keywords $PM_{2.5}$ · Chemical composition · Aerosol acidity · Regional transport · Sanya · Organic markers

Introduction

There have been growing concerns over urban air quality across China in recent decades due to the extremely high aerosol loadings that have accompanied the country's rapid economic development (Zhang et al. 2013; Guan et al. 2014). Atmospheric pollution by particulate matter (PM) with aerodynamic equivalent diameters of $Dp < 2.5$ μm ($PM_{2.5}$) has become a critical issue owing to its effects on climate (IPCC 2013), visibility (Watson 2002), cloud condensation nuclei (CCN) (Seinfeld and Pandis 2006), and cloud, rain, and fog water (Hong et al. 2002). Numerous studies have been conducted in China to investigate $PM_{2.5}$ composition, aerosol physical characteristics, haze formation mechanisms, regional pollution, and environmental effects in large cities, coastal regions, and background sites (Liu et al. 2013, Guo et al. 2014, Pu et al. 2015, Feng et al. 2015, Guo et al. 2017, Zhao et al. 2015a, 2013).

Here, we present the results of a study conducted at Sanya, which is located on the southern end of Hainan Island in the South China Sea and a popular tourist destination. A few studies have been conducted in Sanya to investigate ecological environments, sediment distributions, and meteorological conditions (Li et al. 2013; Qiao et al. 2015), but there has been a lack of comprehensive monitoring of aerosol particles in Sanya or Hainan Island. Recently, (Wang et al. 2015) reported on carbonaceous $PM_{2.5}$ at Sanya, and these authors

Responsible editor: Gerhard Lammel

✉ Jiamao Zhou
zjm@ieecas.cn

✉ Junji Cao
cao@loess.llqg.ac.cn

[1] KLACP, SKLLQG, Institute of Earth Environment, Chinese Academy of Sciences, Xi'an 710061, China

[2] University of Chinese Academy of Sciences, Beijing 100049, China

[3] Division of Atmospheric Sciences, Desert Research Institute, Reno, NV 89512, USA

[4] Hainan Tropical Ocean University, Sanya 572022, China

concluded that there were impacts from a variety of pollution sources in winter while emissions from the burning of fossil fuels were most important in summer. Renowned for its tropical climate, the air quality in Sanya is nearly always better than in most of the Chinese megacities, but occasional pollution episodes do occur there. These affect both air quality and visibility, and they occur most often in wintertime.

The geography of Sanya and its maritime atmosphere make it subject to effects land-sea breeze circulation. The first objective of the work described here was to determine the chemical composition of airborne $PM_{2.5}$ at Sanya during a 1-month intensive monitoring study in winter. We recorded the atmospheric conditions, measured selected chemical components, and characterized transport pathways that can affect the air quality in the area. The Weather Research Forecasting Black Carbon (WRF-BC) model and an organic tracer method were then used to evaluate the contributions of regional emissions to $PM_{2.5}$ at Sanya. Studies of particle formation mechanisms undertaken for the study have led to a better understanding of what controls the aerosol populations, and the results also contribute to the developing national chemical database on $PM_{2.5}$ in China.

Sampling and methodology

Sampling site and methods

Sampling was conducted at the Hainan Tropical Ocean University in the northeastern part of Sanya City, Hainan Province, China (18° 18′ N, 109° 31′ E; Fig. 1) from January 8 to February 8, 2012. Sanya is in the tropical marine monsoon climate zone, and the sampling site itself was is in a suburban area, ~10 km from the South China Sea (Wang et al. 2015).

The sampling equipment was installed on the roof of an academic office building on the campus ~20 m above ground level. Twenty-four hour integrated daily samples (from 10:00 a.m. to 10:00 a.m. in the next day) were collected on 47-mm-diameter quartz-fiber filters (QM/A®, Whatman Inc., UK), and these were used for measurements of carbonaceous aerosols and water-soluble ions. Another set of samples was collected using Teflon®-membrane filters (47 mm, QM/A®, Whatman Inc., UK), and they were used for elemental analyses. Both sets of samples were collected using Airmetrics $PM_{2.5}$ Mini-Volume samplers (Springfield, OR, USA), which operated at flow rates of 5 L min^{-1}. Two blank samples were collected and analyzed to account for any positive artifacts. The sampler was regularly calibrated using a Defender 510 Volumetric Primary Flow Standard (Bios International Corporation, Butler, NJ, USA). The variance in flow was approximately ±2%. All of the samples were properly stored in a freezer at 4 °C until analysis to prevent any loss of volatile matter. Meteorological data were provided by the Sanya Meteorology Administration.

Chemical analyses

Mass measurements

For the mass measurements, the Teflon® filters were equilibrated at a temperature between 20 and 23 °C and relative humidity (RH) of 35–45% for at least 24 h, and the masses of the filters were determined be weighing the filters before and after the samples were collected. A Sartorius MC5

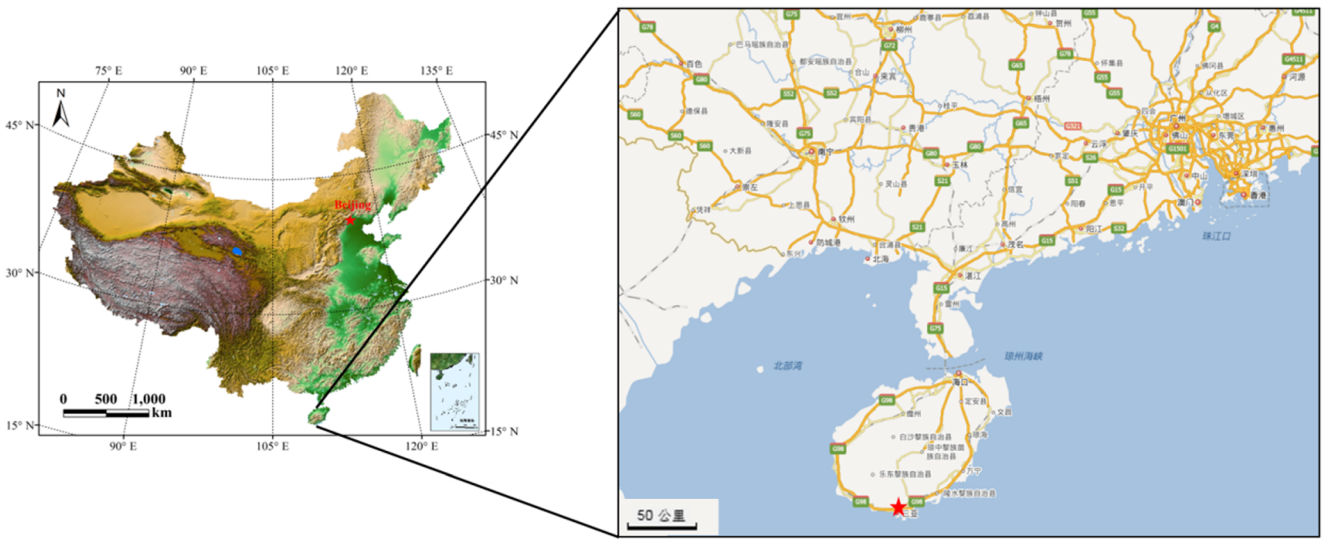

Fig. 1 Location of the sampling site in Sanya, China

electronic microbalance with ± 1 μg sensitivity (Sartorius, Gottingen, Germany) was used for the mass determinations. Each filter was weighed at least three times, and the net mass was obtained by subtracting the difference between the averaged pre- and post-sampling weights.

Carbonaceous aerosol analysis

Prior to sampling, all of the quartz-fiber filters were preheated in a furnace at 800 °C for 3 h to remove any contaminants, and both before and after sampling, the filters were stored in the freezer at < 4 °C. The carbon analyses were carried out using a Desert Research Institute (DRI) Model 2001 carbon analyzer (Atmoslytic Inc., Calabasas, CA, USA) following the IMPROVE_A thermal/optical reflectance (TOR) protocol (Chow et al. 1993; Chow et al. 2004). A punch aliquot of each quartz filter sample was heated in a stepwise manner to obtain data for four organic carbon (OC) fractions (OC1, OC2, OC3, and OC4 in a helium atmosphere at 140, 280, 480, and 580 °C), and three elemental carbon (EC) fractions (EC1, EC2, and EC3 in a 2% oxygen/98% helium atmosphere at 580, 740, and 840 °C). Pyrolyzed carbon (OP) was produced at < 580 °C in the inert atmosphere, and the decrease in reflected light caused by OP was used to correct for charred OC. Total OC was defined as the sum of OP plus the four OC fractions, and total EC was the sum of the three EC fractions minus OP.

Elemental analysis

The concentrations of 40 elements (Na, Mg, Al, Si, P, S, Cl, K, Ca, Sc, Ti, V, Cr, Mn, Fe, Co, Ni, Cu, Zn, Ga, As, Se, Br, Rb, Sr, Y, Mo, Pd, Ag, Cd, Sn, Sb, Cs, Ba, La, W, Au, Hg, Pb, and Tl) on the Teflon® filters were measured by energy dispersive x-ray fluorescence (ED-XRF) spectrometry (Epsilon 5 ED-XRF, PANalytical B.V., the Netherlands). The spectrometer used a three-dimensional polarizing geometry with 11 secondary targets (i.e., CeO_2, CsI, Ag, Mo, Zr, KBr, Ge, Zn, Fe, Ti, and Al) and one target (Al_2O_3) that resulted in high signal-to-noise ratios and low detection limits (Watson et al. 1999). The X-ray source was a side-window X-ray tube with a gadolinium anode that operated at a current of 0.5 to 24 mA and an accelerating voltage of 25 to 100 kV (maximum power 600 W). The characteristic X-ray radiation was detected by a germanium detector (PAN 32). Each filter sample was counted for 30 min.

Ion analysis

One quarter of each quartz-fiber sample filter was cut using and extracted in 10 ml of high-purity water. Ten major ions (Na^+, NH_4^+, K^+, Mg^{2+}, Ca^{2+}, NO_3^-, SO_4^{2-}, Cl^-, F^-, and Br^-) were measured with a DX600 ion chromatograph (Dionex Inc., Sunnyvale, CA, USA) (Chow and Watson 1999). A CS12 column (150 × 4 mm) and an AS14 column (150 × 4 mm) were used for chromatographic separations of cations and anions analyses, respectively. The mothd details can be found in (Zhang et al. 2011).

Organic speciation

Non-polar organic compounds, including polycyclic aromatic hydrocarbon (PAHs), alkanes, and hopanes, were measured on the quartz-fiber filter using in-injection port thermal desorption-gas chromatography/mass spectrometry (TD-GC/MS). The sensitivity of TD-GC/MS method is much better than the traditional solvent extraction approach, and the thermal desorption method also requires less labor and uses less chemicals (Chow et al. 2007). The experimental procedures we used have been described in detail by Ho and Yu (2004)), Ho et al. (2008)), and Ho et al. (2011)). In brief, a filter aliquot (0.5–1.0 cm^2) was cut and thermally extracted inside the GC injector port (GC 6890, Agilent Technology, Inc., Santa Clara, CA, USA) at 275 °C. The desorbed organic compounds were separated with a capillary column and detected by a MS detector (m/z 50–550) (MS 5975, Agilent Technology, Inc.).

Quality assurance and quality control (QA/QC)

The limit of detections (LODs) and relative errors for carbonaceous aerosol, water-soluble ions, and elemental components are shown in Table 1. The LOD is defined as the amount of an analyte that generates an analytical signal equal to the sum of the mean blank signal plus three times the standard deviation of the blank signals (Meier and Zünd 2005).

QA/QC procedures have been described in detail for the carbon analysis (Cao et al. 2003), elemental analyses (Xu et al. 2012, 2016), and ion chromatographic measurements (Shen et al. 2009a, b; Zhang et al. 2011). The QA/QC procedures for the organic species analyzed by TD-GC/MS also have been described elsewhere (Ho et al. 2008, 2011). Replicate analyses were done for each group of ten samples. Blank filters were also analyzed, and the sample results were corrected for the average of the blank concentrations.

Non-sea salt sulfate calculation

Sea salt sulfate ($ssSO_4^{2-}$) and non-sea salt sulfate ($nssSO_4^{2-}$) were calculated by assuming that Na^+ was only from by sea salt and multiplying the measured Na^+ by the seawater SO_4^{2-}/Na^+ mass ratio of 0.25 as follows:

$$ssSO_4^{2-} = 0.25 \times Na^+ \quad (1)$$

$$nssSO_4^{2-} = SO_4^{2-} - ssSO_4^{2-} \quad (2)$$

Table 1 Limit of detection and relative error of analysis methods for carbonaceous aerosol, water-soluble ions, and selected elemental components

Species	Limit of detection (μg ml^{-1})	Relative error	Species	Limit of detection (μg cm^{-2})	Relative error
F^-	0.0094	0.98%	OC	0.39	2.95%
Cl^-	0.0087	1.04%	EC	0.01	5.43%
NO_2^-	0.0050	2.15%	TC	0.40	0.74%
Br^-	0.0290	3.39%	Ti	0.005	2.98%
NO_3^-	0.0256	2.41%	Mn	0.015	10.23%
SO_4^{2-}	0.0270	2.93%	Fe	0.018	4.60%
Na^+	0.0005	2.18%	Zn	0.005	18.66%
NH_4^+	0.0010	2.08%	As	0.006	8.90%
K^+	0.0011	2.14%	Br	0.005	20.10%
Mg^{2+}	0.0008	0.91%	Pb	0.023	8.22%
Ca^{2+}	0.0012	2.18%	Al	0.043	8.79%

Thermodynamic model

Acidity is one of the most important factors that determine the aerosols' physical and chemical properties. Investigations of in situ aerosol properties and how they vary in relation to acidity and water content are fundamental to assessing their involvement in heterogeneous reactions, especially nitrate formation (Pathak et al. 2009). Many researchers (Zhang et al. 2000; Pathak et al. 2004; Zhang et al. 2007; Pathak et al. 2009; Engelhart et al. 2011; Pathak et al. 2011; Squizzato et al. 2013) have applied the Extended Aerosol Inorganic Model (E-AIM, http://www.aim.env.uea.ac.uk/aim/aim.php) to simulate the in situ aerosol acidity ($[H^+]_{Free}$), the activities of ionic species in aqueous aerosols, and the solid- and liquid-phase composition of the aerosol (Clegg et al. 1998). In this study, a recent version of the E-AIM model IV (E-AIM4, (Friese and Ebel 2010) was used to simulate the acidity and thermodynamic properties of the H^+–NH_4^+–Na^+–SO_4^{2-}–NO_3^-–Cl^-–H_2O mixture in $PM_{2.5}$. The average ambient temperature, relative humidity (RH), and molar concentrations of total aerosol acidity ($[H^+]_{Total}$) were input into E-AIM4 to obtain $[H^+]_{Free}$ and the number of moles of selected chemical species in the aqueous phase. In this study, $[H^+]_{Total}$ was estimated using the ionic balance of the dominant inorganic ionic species (Lippmann et al. 2000; Pathak et al. 2009); these include sulfate, nitrate, chloride, ammonium, and sodium.

$$[H^+]_{Total} = 2SO_4^{2-} + NO_3^- + Cl^- - \left(NH_4^+ + Na^+\right) \quad (3)$$

Results and discussion

Time series of meteorological conditions and $PM_{2.5}$

Meteorological data provided by Sanya Meteorology Administration showed that the prevailing winds during study were northeasterly, and a time series plot shows that the wind speed was relatively constant over the course of the study (Fig. 2). The average wind speed, temperature, and relative humidity (RH) were 0.6 ± 0.2 ms^{-1}, 22.5 ± 1.4 °C, and 90.9 ± 5.6%, respectively. The daily concentrations of $PM_{2.5}$ ranged from 8.6 to 35.3 μg m^{-3}, and the arithmetic mean $PM_{2.5}$ mass was 20.4 μg m^{-3}. Four typical periods, that is, two episodes with high $PM_{2.5}$ (identified with red rectangles in Fig. 2) and two episodes with low $PM_{2.5}$ (shown in blue rectangles), were selected for discussion. We found that higher $PM_{2.5}$ mass concentrations occurred when the winds were from the north-northeast wind and the RH was low. Lower $PM_{2.5}$ loadings occurred when the winds were south or southwesterly and the RH was high. These results show that fine particles at Sanya are affected by wind direction, which in turn implies that transport affects the aerosol. More discussion of the daily changes in $PM_{2.5}$ is presented below.

$PM_{2.5}$ chemical composition

The $PM_{2.5}$ mass concentrations and those of chemicals that mostly concerned are shown in Table 2. The $PM_{2.5}$ mass and chemical species concentrations at Sanya were obviously lower than those in other Chinese coastal cities including Hong Kong, Qingdao, Shanghai, Xiamen, and Guangzhou where the same analytical methods were used (Cao et al. 2012). The concentrations of $PM_{2.5}$, carbonaceous aerosol, water-soluble aerosol, and elemental components also were lower compared with a group of coastal cities (13 cities) along the Western Taiwan Straits region. The $PM_{2.5}$ mass concentrations were below the 24-h limits of 75 μg m^{-3} promulgated by the Chinese National Environmental Protection Agency, and they also were lower than the recommended levels established by other countries and international health organizations. The good air quality at Sanya can be explained by the relatively small population of ~ 500,000 and limited impacts from anthropogenic pollution sources, such as heavy

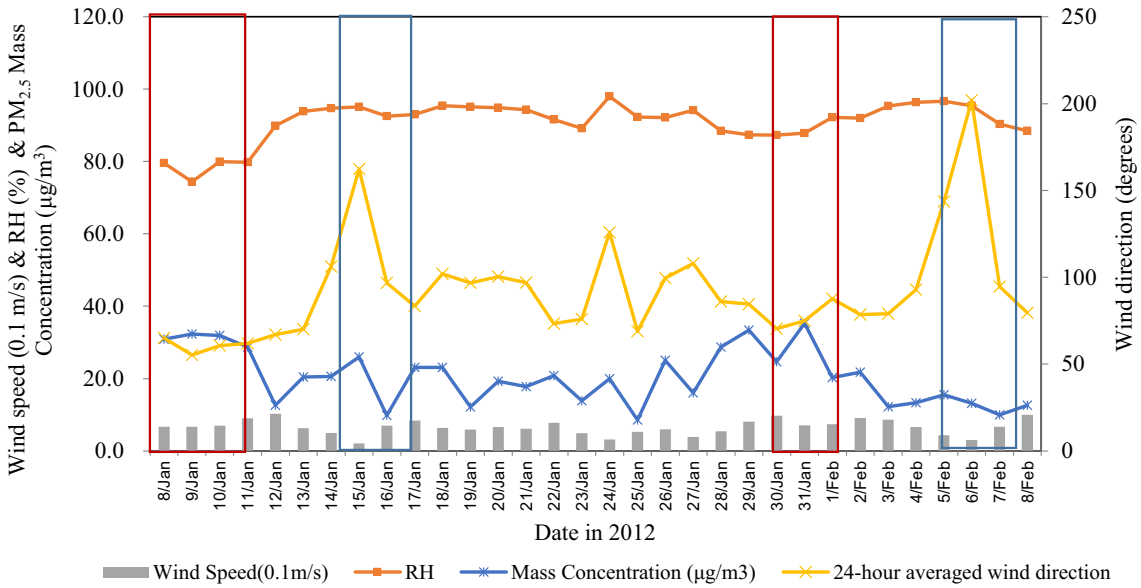

Fig. 2 Time series of meteorological conditions and $PM_{2.5}$ concentrations

industries. Tourism is a pillar industry in Sanya and that has small to environmental impacts other than limited emissions from local transport and vehicles used for tourism. In addition, the geographical location of Sanya is favorable: the land breeze-sea breeze circulation prevails (Fig. 1), and meteorological conditions are generally conducive to pollutant dispersal.

The geography and climate at Sanya have a degree of similarity with Hong Kong where a comprehensive study on atmospheric fine particle was conducted (Cao et al. 2012). In Hong Kong, seasonal variations in $PM_{2.5}$ were apparent, and high loadings of various chemical components were found in winter. However, the concentration differences of most species (e.g., means of OC and EC) between summer and winter were vanishingly small in Sanya (Wang et al. 2015). The lack of seasonality can be ascribed to the consistency of local pollution inputs. In addition, the concentrations of several chemicals, including Ti and Fe, were very low in Sanya, much closer to the levels in Hong Kong in summer than in the more polluted winter. These results simply indicate that there were different pollution sources for the two cities even though both are located on coastlines.

Aerosol mass balance

A material balance for the aerosol was calculated to rank the mass contributions of important marker species (Fig. 3). The order of importance was organic matter (OM) > nss-sulfate (nss-SO_4^{2-}) > geological material (GM) > EC > nitrate (NO_3^-) > sea salts > ammonium (NH_4^+). Due to the low concentrations, several chemical components in some samples were not detected, including Cl^-, NO_2^-, Na^+, NH_4^+, and K^+ which had limits of detection of 0.0087, 0.0050, 0.0005, 0.0010, and 0.0011 μg ml^{-1}, respectively. The average concentrations for those analytes were calculated by substituting half of the LOD for the undetected samples to avoid overestimation of the concentrations.

Approximately 21.0% of the $PM_{2.5}$ mass was not identified. This value is higher than the results shown by (Cao et al. 2012) and that may have been due to underestimations of the weighting factors for certain components or uncertainties in the gravimetric measurements. For example, the OM would have underestimated if the non-quantified mass ratio of 1.6 that was used in the calculations is not representative of the OM at Sanya. In fact, the lush vegetation at Sanya and surrounding areas may provide precursors for secondary aerosol formation, including OM, and the photochemical reactions at the site would be favored by the high temperatures and strong solar radiation (Wang et al. 2015). Andrews et al. (2011) also found that 28–42% of the $PM_{2.5}$ collected in national park could not be identified, attributed to the formations of multifunctional organic compounds. GM accounted for 17.8% of the $PM_{2.5}$ mass in Sanya compared with 12 to 34% at 14 Chinese megacities (Cao et al. 2012). This type of material is typically due to soil and dust re-suspension, construction projects, and agricultural activities. A relatively high contribution of GM at Sanya can be explained by the fact that an active construction site was next to the sampling location during the study. The relative abundances of other fractions were consistent with the results for other cities, including Beijing, Shanghai, Guangzhou, and Chongqin (Cao et al. 2012; Zhao et al. 2013), where OM and nss-SO_4^{2-} were two major PM components. At Sanya, OM and nss-SO_4^{2-} accounted for 24.5 and 20.5%, respectively, of the total PM mass.

Oxidation-reduction reactions involving H_2O_2 contribute to sulfate formation in the aqueous phase, particularly when the pH is below 5 (Chandler et al. 1988; Das and Aneja 1994;

Table 2 $PM_{2.5}$ mass and chemical composition for Sanya, coastal megacities, and a coastal city group (13 medium and small cities) along the Western Taiwan Straits Region (WTSR) (μg m^{-3})

Parameter or species	Sanya[a]	Sanya[b]	Hong Kong[c]	Hong Kong[c]	Qingdao[c]	Shanghai[c]	Xiamen[c]	Guangzhou[c]	Coastal cities in WTSR[d]
Sampling time	2012	2013	2003	2003	2003	2003	2003	2003	2010, 2011
Season	Winter	Summer	Winter	Summer	Winter	Winter	Winter	Winter	Winter
$PM_{2.5}$	20.4 ± 7.6	n.a.	88.4 ± 23.1	30.4 ± 7.3	134.8 ± 43.0	139.4 ± 50.6	74.2 ± 27.2	110.2 ± 79.6	102.9 ± 37.7
OC	3.1 ± 1.3	3.2 ± 0.9	13.3 ± 5.1	6.6 ± 1.9	26.3 ± 10.3	26.7 ± 7.7	15.5 ± 5.7	24.2 ± 22.1	13.8 ± 3.4
EC	1.2 ± 0.4	0.9 ± 0.2	6.9 ± 2.8	3.3 ± 1.1	6.2 ± 2.5	8.6 ± 2.0	4.9 ± 1.5	8.4 ± 6.6	2.7 ± 0.9
SO_4^{2-}	4.2 ± 2.6	n.a.	21.4 ± 5.6	4.3 ± 1.2	21.1 ± 7.7	21.6 ± 12.3	13.5 ± 8.4	20.6 ± 10.8	13.66
NO_3^-	1.2 ± 0.6	n.a.	9.5 ± 2.7	1.2 ± 0.5	19.3 ± 9.2	17.5 ± 8.7	7.6 ± 4.1	11.5 ± 7.8	13.27
Ca^{2+}	0.6 ± 0.4	n.a	n.a	n.a	n.a	n.a	n.a	n.a	1.00
NH_4^+	0.4 ± 0.6	n.a.	8.0 ± 3.5	0.3 ± 0.2	15.3 ± 5.2	14.5 ± 5.9	7.0 ± 3.9	8.5 ± 7.6	8.03
Na^+	0.3 ± 0.4	n.a.	0.6 ± 0.5	0.72 ± 0.3	3.2 ± 1.6	1.9 ± 1.3	0.8 ± 0.6	1.5 ± 1.6	0.43
K^+	0.3 ± 0.2	n.a.	0.8 ± 0.4	0.6 ± 0.1	2.8 ± 1.3	2.1 ± 1.1	0.9 ± 0.5	1.8 ± 1.2	1.44
Cl^-	0.3 ± 0.2	n.a.	1.2 ± 1.5	1.2 ± 0.4	6.5 ± 2.2	6.6 ± 3.1	1.4 ± 0.5	1.9 ± 2.0	2.17
Al	0.24 ± 0.11	n.a.	n.a.	n.a.	n.a.	n.a.	n.a.	n.a.	n.a.
Ti	< LD	n.a.	0.05 ± 0.03	0.04 ± 0.02	0.09 ± 0.02	0.09 ± 0.02	0.06 ± 0.02	0.06 ± 0.03	n.a
Mn	0.02 ± 0.01	n.a	0.04 ± 0.03	0.04 ± 0.04	0.09 ± 0.05	0.18 ± 0.07	0.05 ± 0.01	0.06 ± 0.04	n.a
Fe	0.05 ± 0.03	n.a.	0.62 ± 0.15	0.27 ± 0.11	0.95 ± 0.28	1.18 ± 0.38	0.60 ± 0.10	0.78 ± 0.51	n.a
Zn	0.02 ± 0.02	n.a.	0.35 ± 0.19	0.19 ± 0.15	0.43 ± 0.23	0.93 ± 0.39	0.71 ± 0.31	0.59 ± 0.32	0.52
As	< LD	n.a	0.01 ± 0.01	0.01 ± 0.00	0.02 ± 0.01	0.03 ± 0.01	0.02 ± 0.01	0.04 ± 0.02	n.a
Br	< LD	n.a	0.01 ± 0.01	0.01 ± 0.00	0.17 ± 0.12	0.05 ± 0.01	0.02 ± 0.01	0.06 ± 0.04	0.04
Pb	0.02 ± 0.01	n.a.	0.19 ± 0.09	0.01 ± 0.02	0.27 ± 0.15	0.48 ± 0.17	0.22 ± 0.11	0.42 ± 0.26	0.11

n.a. not available, < *LD* the value below the limit of detections

[a] This study. Both F^- and Br^- were measured but below the detection limit, so they were not listed in the comparison table

[b] Wang et al. (2015)

[c] Cao et al. (2012)

[d] Yin et al. (2014), Niu et al. (2013), Xu et al. (2013)

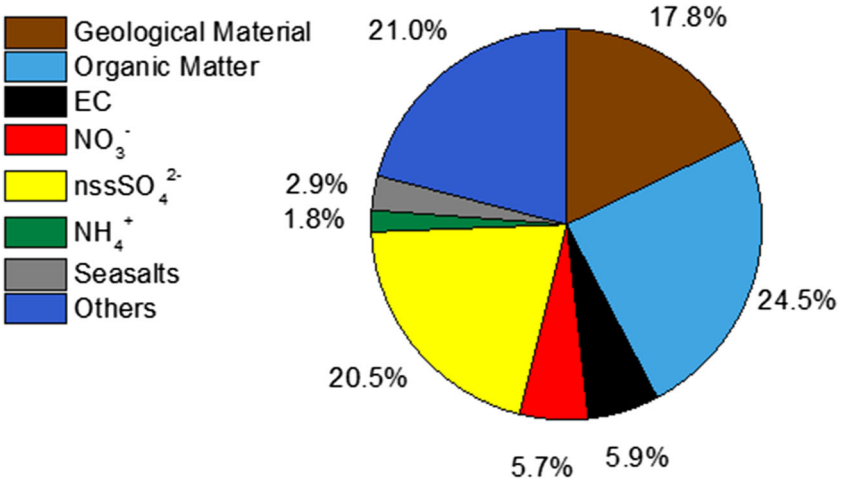

Fig. 3 Chemical composition of $PM_{2.5}$ from Sanya. Organic matter was estimated as 1.6 × OC (El-Zanan et al. 2005; Chen and Yu 2007; El-Zanan et al. 2012) to account for the unmeasured hydrogen and oxygen. Geological material was estimated as Al/0.07 (Zhang et al. 2003). Sea salts were estimated as $Cl^- + (1.4486 \times Na^+)$ where 1.4486 is the ratio of the concentration of all elements in sea water except Cl^- to the concentration of Na^+ (Li et al. 2010)."Others" was the remaining unaccounted-for mass after subtracting the sum of measured components from the $PM_{2.5}$ mass. Unaccounted-for mass may be composed of unmeasured geological material (e.g., calcium carbonate), OM with a higher than assumed fraction of oxygen, residual water, and other unmeasured species. Uncertainties in gravimetric analyses also could introduce errors

Fung et al. 1991; He et al. 2010; Meagher et al. 1990), and the results indicate that high RH greatly promoted the oxidation of sulfur dioxide (SO_2) to SO_4^{2-}. Sea salt was estimated to be 3.67% of the $PM_{2.5}$ mass, and therefore, sea salt SO_4^{2-} was almost negligible, accounting for only 0.34% of $PM_{2.5}$ mass. The relatively low value for sea salt is close to the contributions of 4.2 and 5.0% reported at the urban sites of Borgerhout (Bencs et al. 2008). However, the small sea salt proportion in the atmosphere of Sanya can be explained, at least in part, by the seasonality of the prevailing winds; that is, northeasterly winds prevail in winter, and therefore, the aerosol is mainly influenced by air masses from the mainland. The phenomenon of "chlorine loss" (Ohta and Okita 1990) and multivariate analysis (Thurston and Spengler 1985) of the data for water-soluble ions showed that sea salts were significantly impacted by the sea breeze while the secondary salts, like sulfate, were mainly contributed by land breeze. It is also supported by the mean value $[Cl^-]/[Na^+]$ (0.42 in this study) which is lower than the value in the sea water (1.16) (Keene et al. 1986).

Ammonium ion had an average concentration of 0.4 ± 0.6 μg m^{-3}, and it accounted for only 1.8% of the $PM_{2.5}$ mass and was undetectable in 32 samples. Animal manure and fertilizer applications are well-known sources for ammonia (NH_3) (Cui et al. 2013; Gu et al. 2014), but the results indicate there was relatively little ammonium from these sources around Sanya. Other anthropogenic, non-agricultural sources for NH_3, such as motor vehicles, fuel combustion, and landfills also exist, but their impact apparently was small (Pierson and Brachaczek 1983; Sutton et al. 2000; Battye et al. 2003; Wilson et al. 2004; Sutton et al. 2008). As noted above, tourism is the main industry in Sanya, and emissions from the industrial and agricultural sectors are relatively small.

Wu et al. (2016)) used annual girded emissions data to construct and annual Chinese NH_3 emission map from 2001 to 2008.The annual NH_3 emission for the Hainan Province was only 0.5–2.1 t km^{-2} mol km^{-3}, which was consistent with our results showing low ammonium levels. Due to its short atmospheric lifetime, NH_3 typically deposits on surfaces near the source regions (Walker et al. 2004). As the primary gaseous base in the atmosphere, NH_3 influences the acidity of solid- and aqueous-phase aerosol species, cloud water, and precipitation. Ammonia may be either wet- or dry-deposited as a gas or react with sulfuric (H_2SO4), nitric (HNO_3), nitrous acid (HONO), and hydrochloric acid (HCl) to form ammonium sulfate $[(NH_4)_2SO_4]$, bisulfate (NH_4HSO_4), nitrate (NH_4NO_3), nitrite (NH_4NO_2), and chloride (NH_4Cl) aerosols. The Pearson correlation coefficient calculated for NH_4^+ and SO_4^{2-} at Sanya was 0.94 followed by 0.69 for and NO_2^- and 0.64 for NH_4^+ and NO_3^-. These correlations suggest that NH_4^+ preferentially neutralizes H_2SO_4, which has a relatively low vapor pressure. However, when ammonium concentrations are low and neutralization ratios are small, therefore, other anions can neutralize the residual acids by forming sodium, potassium, calcium, and magnesium salts.

Aerosol acidity

Two important parameters commonly used to represent the aerosol acidity. The first is total acidity ($[H^+]_{Total}$), which is defined as the total amount of the deliquesced aerosol acid measured as strong acids, including sulfuric, nitric, and chloric

acid (Li et al. 2014) and calculated by the method described in the "Thermodynamic model" section. The second parameter, in situ acidity $[H^+]_{Free}$, is the actual acidity of aerosol, which is influenced by the chemical and photochemical reactions in the atmosphere and included in E-AIM model IV. The average $[H^+]_{Total}$ and $[H^+]_{Free}$ calculated by the thermodynamic method were 168.2 ± 84.8 and 108.9 ± 50.8 nmol m^{-3}, respectively. These values are lower than what has been reported for megacities such as Beijing and Shanghai, but they are higher than those at Guangzhou and Lanzhou in summer (Pathak et al. 2009). In addition, the aerosol at Sanya was more acidic than that estimated for Xiamen, another coastal city, in winter (Wu et al. 2017). It is noteworthy that $[H^+]_{Free}$ accounted for 64.7% of $[H^+]_{Total}$. The proportion is almost double the averages measured in the five cities referenced above. Aerosol acidities can vary over a wide range for different source materials, either anthropogenic or natural, and they can be affected by regional emissions and weather conditions. Higher water contents in aerosol particles can promote the uptake of sulfur dioxide (SO_2), H_2SO_4, and HNO_3; this can accelerate SO_2 oxidation and increase the formation of H_2SO_4 in the liquid phase. To summarize, the warm and humid climate at Sanya likely supported heterogeneous reactions that led to the formation of sulfate, and the high acidity can be explained by the high aerosol SO_4^{2-} combined with the limited local NH_3 emissions and high RHs (on average 91.9%).

The E-AIM model IV (E-AIM4) only considers the major water-soluble ions in the atmosphere; these include NH_4^+, Na^+, SO_4^{2-}, NO_3^-, and Cl^- but not Ca^{2+}, K^+, or Mg^{2+}. However, these latter ions cannot be ignored at the Sanya site, and therefore, the acidity estimated by E-AIM4 may not be accurate. A linear equation between cation and anion is given as

$$[\text{Cation}] = 0.68 \times [\text{Anion}] + 0.001 \quad (4)$$

by using the formula

$$\text{Cation equivalent} = \frac{Na^+}{23} + \frac{NH_4^+}{18} + \frac{K^+}{39} + \frac{Mg^{2+}}{12} + \frac{Ca^{2+}}{20} \quad (5)$$

$$\text{Anion equivalent} = \frac{SO_4^{2-}}{47} + \frac{NO_3^-}{62} + \frac{Cl^-}{35.5} + \frac{Br^-}{80} + \frac{F^-}{19} \quad (6)$$

where [cation] and [anion] are expressed in normality. Calculation of the cation and anion balance was used to support for the findings regarding aerosol acidity in Sanya City.

Moreover, the acidity ratio (Engelhart et al. 2011) or neutralization ratio (NR) (Bencs et al. 2008) can be defined as

$$NR = \left([NH_4^+]\right) / \left[SO_4^{2-}\right] + \left[NO_3^-\right] \quad (7)$$

which is a way of expressing the degree of neutralization of sulfate and nitrate by ammonium (expressed in equivalents). That is, NR indicates the aerosol acidity characteristics by accounting for the possible neutralization of only the two major inorganic acids (nitric and sulfuric) with ammonium. In $PM_{2.5}$, NR < 1 typically indicates the partial neutralization of acidic aerosols. The NR in Sanya was much less than unity, indicating limited neutralization, and it also lower than the values calculated for other megacities (Pathak et al. 2009; Fu et al. 2015; Wu et al. 2017). Various atmospheric chemical and physical processes affect the acidity of the aerosol. For example, at Beijing and Shanghai, NH_3 neutralized 40–50% of SO_4^{2-} and NO_3^-, and a complete neutralization was seen in Lanzhou and Guangzhou (Pathak et al. 2009). Such neutralization evidently did not occur at Sanya because NR was only 0.18 due to an insufficient supply of ammonia.

The NR ratio was highly correlated with the free acidity ($R^2 = 0.77$) as shown in Fig. 4, and the degree of neutralization increased with free acidity. In contrast, Fu et al. (2015) and Wu et al. (2017) found that NR values decreased when free acidities increased at Guangzhou and Xiamen in winter, and furthermore, the relationship for those sites was logarithmic. Sanya, Guangzhou, and Xiamen are all near the sea, but the local pollution emissions at the latter two sites are much higher than those in Sanya, and this is a likely reason the aerosol acidity differed among the sites. Positive correlations between the degree of neutralization and free acidity were likely the result of the conversion of SO_2 to SO_4^{2-} through aqueous reactions, but as discussed below, there it is also likely that the correlations were driven by regional emission and transported to the sampling site.

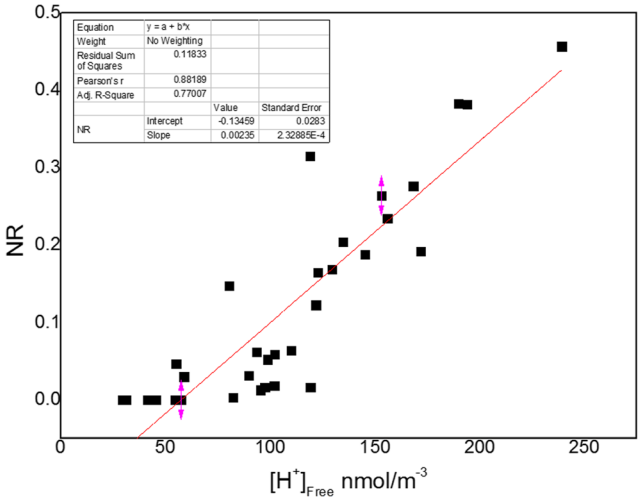

Fig. 4 Relationship between neutralization ratio and free acidity

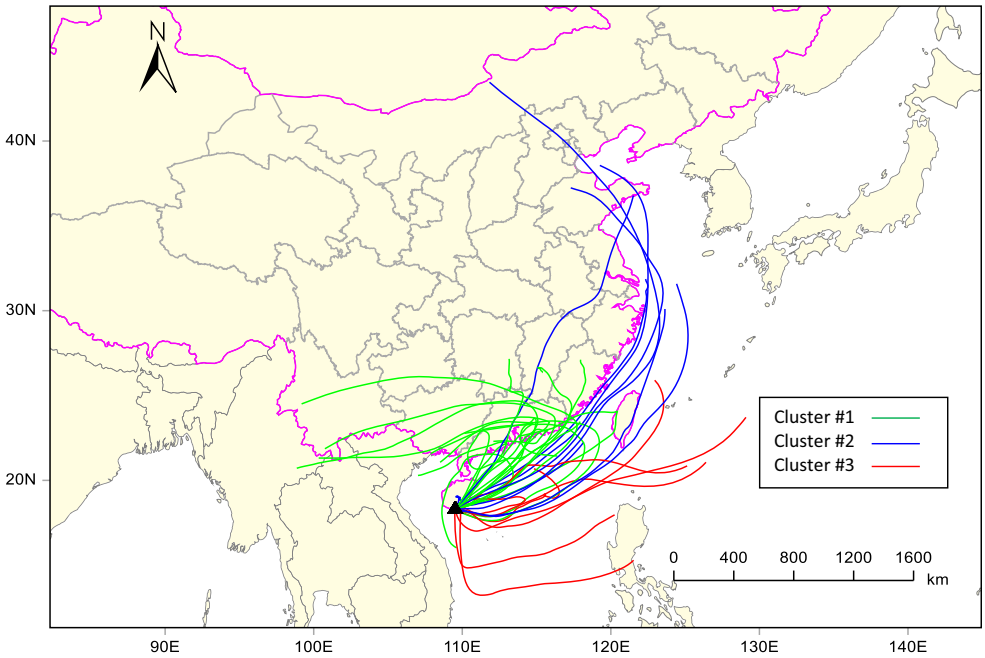

Fig. 5 Three-day air-mass trajectories calculated backwards in time reaching Sanya at 500 m above ground every hour during the campaign period and their grouping into three trajectory clusters

Regional scale transport

Clusters of air-mass trajectories

Even though local pollution sources, such as motor vehicle emissions, normally are the main sources for the aerosol at Sanya (Wang et al. 2015), potential impacts from regional emissions are worth evaluating. Pollutant transport to the site is mainly driven by synoptic winds, local sea-land breeze circulation, and orographic effects. Three-day air-mass trajectories, calculated backwards in time and reaching at Sanya at 500 m above ground level were calculated for every hour during the campaign by using the National Oceanic and Atmospheric Administration (NOAA) Air Resource Lab (ARL) Hybrid Single-Particle Lagrangian Integrated Trajectory (HYSPLIT) model and gridded meteorological data (Global Data Assimilation System, GDAS1) (www.arl.noaa.gov/HYSPLIT_pubs.php) (Stein et al. 2015).

Most of the air masses came from east and northeast during the sampling period (Fig. 5), and this is consistent with the wintertime climatology. The underlying premise for evaluating transport pathways is that air masses pass over potential source areas and accumulate aerosols and their precursors before they arrive at the receptor site. The air masses were grouped into three clusters according to their origin (Fig. 5). The average concentrations of chemical species and parameters for the three clusters are summarized in Table 3.

As shown in Fig. 5, 16 trajectories were grouped into cluster 1: this group primarily originated over South Asia and South China, and it had the highest average $PM_{2.5}$ concentration (26.5 μg m^{-3}) of the three clusters. There were ten trajectories associated with cluster 2 which primarily originated from eastern coastal regions and the East China Sea, and these had the lowest average $PM_{2.5}$ concentration of the clusters (13.9 μg m^{-3}). The remaining six trajectories were grouped into cluster 3, and that group, which had an intermediate $PM_{2.5}$ loading of 15.2 μg m^{-3}, originated from the South China Sea or the ocean and then passed over the South China Sea.

The trajectories were classified as "polluted" if the $PM_{2.5}$ concentration for the sample matched to the trajectory (you might briefly describe how were the samples matched to the trajectories) was higher than the average value of 20.4 μg m^{-3}. Otherwise, if the $PM_{2.5}$ loading for a sample was below the average the trajectory was identified as "normal." Based on this approach, 13 days with trajectories in cluster 1 were classified as "polluted." No polluted day were found for clusters 2 or 3, demonstrating that the air quality was better when the flow was from eastern coastal regions or the South China Sea. This supports our conclusion that the air masses that passed over southern Asia and South China were the main regional pollution sources for Sanya.

In addition to the $PM_{2.5}$ mass loadings, the concentrations of various chemical species showed different rankings among the three clusters. Cluster 1, which had all of the "polluted" trajectories, had the highest concentrations of OC and secondary inorganic aerosol (SIA) compounds such as SO_4^{2-}, NO_3^-, and NH_4^+, and the highest values for $[H^+]_{Total}$, $[H^+]_{Free}$, and NR. The high concentrations of these species show that the transport pathways represented by this cluster were associated with the worst air quality at the receptor site, and those effects can be traced to pollutant emissions from southern Asia. Meanwhile, cluster 3 had the highest concentration of Na^+ and Cl^-, which are major components of sea salt, and

Table 3 Characteristics of three trajectory clusters and $PM_{2.5}$, species concentrations, and parameters grouped by cluster

	Cluster 1 Origin	Cluster 2	Cluster 3
Variable	South Asia and South China	Eastern coastal region	South China Sea
Number of trajectories	16	10	6
Polluted trajectories	13	0	0
Mass, μg m^{-3}	26.5	13.9	15.2
Organic carbon, μg m^{-3}	3.8	2.5	2.5
Elemental carbon, μg m^{-3}	1.4	0.9	1.0
nssSO_4^{2-}, μg m^{-3}	5.8	2.1	3.7
NO_3^-, μg m^{-3}	1.4	0.8	1.0
NH_4^+, μg m^{-3}	0.7	0.04	0.1
Cl^-, μg m^{-3}	0.2	0.2	0.4
Na^+, μg m^{-3}	0.4	0.3	0.8
$[H^+]_{Total}$, nmol m^{-3}	220.8	93.4	136.4
$[H^+]_{Free}$, nmol m^{-3}	143.0	64.8	91.7
Neutralization ration, unitless	0.2	0.02	0.04
Relative humidity, %	0.88	0.85	0.93
Temperature, °C	18.5	17.8	19.4

therefore, this cluster appears the most representative of marine air. Dimethyl sulfide (DMS), produced by marine phytoplankton, is one of the major natural sources of atmospheric sulfate, and methanesulfonic acid (MSA) and non-sea salt of SO_4^{2-}, which are oxidation products of DMS, are two major contributors to natural aerosol acidity (Andreae and Barnard 1984; Nguyen et al. 1992; Yang et al. 2011). The mixing of marine air with the local aerosols likely led to the comparatively high concentrations of SO_4^{2-}, $[H^+]_{Total}$, and $[H^+]_{Free}$ in cluster 3, but their sources and ways in which they formed were different from those in cluster 1.

The lengths of the trajectories are indicative of transport speed; that is, a longer pathway equates to a faster transport. The trajectories grouped into cluster 2 passed over the Eastern China and the East China Sea, and they had the longer lengths compared with those in the other two clusters. The trajectories in cluster 2 also were associated with cold air and strong winds, which would be conducive to convection and promote the dispersal of pollutants, leading to good air quality in Sanya. Cluster 2 would be subject to atmospheric removal process like dry and wet depositions during long-range transport. Overall, the $PM_{2.5}$ aerosol in Sanya was incompletely neutralized and thus acidic, but the samples for clusters 2 and 3 had lower neutralization ratios than those in cluster 1, indicating relatively less NH_3 and NH_4^+ for those pathways.

A case study of high $PM_{2.5}$

To investigate the sources for $PM_{2.5}$, we focused on an episode at Sanya on 31 January 2012 and the day before the episode and day after it. The filter samples for the 31 January episode were assigned to cluster 1, and the concentrations of pollutants in that sample were significantly higher compared with the averages for the other sampling days. The increases over average were as follows: NH_4^+ (404%) > SO_4^{2-} (167%) > OC (140%) > K^+ (108%) > NO_3^- (102%) > EC (85.9%) > $PM_{2.5}$ mass (72.7%). Three-day back trajectories for the episode showed the air masses originated from the middle of China, passed along with Pearl River Delta (PRD) region, and finally arrived at Sanya on the day of the episode.

To apportion the potential pollution sources for this episode, a simplified Weather Research and Forecasting chemistry (WRF-Chem) model was run in conjunction with the (WRF) model. WRF is a numerical weather prediction system and widely used in both operational forecasting and atmospheric research. Detailed descriptions of the WRF model have been reported elsewhere (www.wrf-model.org/index.php). In addition to the standard features, EC has been added as a chemical tracer in the WRF-EC model (Zhao et al. 2015b), and it was used to track the long-range transport of EC from source regions to the sample area.

EC is useful as a tracer for atmospheric transport because it is directly emitted from combustion sources and has relatively low chemical reactivity (Zhao et al. 2015b; Cao et al. 2013). The complex chemical schemes for gases and aerosols in the standard WRF-Chem model rely on modules that perform online calculations of dynamic inputs (e.g., winds, temperature, boundary layer); adjective, convective, and diffusive transport; dry deposition; tracer particles; and surface emissions. The newly added calculations for EC use an emission inventory obtained from (Streets et al. 2003). The horizontal resolution of the model was set at 3 × 3 km in a 450 × 300 km domain centered on Sanya for our study.

The EC simulated with the WRF-EC model was generally consistent with the measured EC, suggesting the WRF-EC model was able to capture the sources and processes responsible for the variability in the concentrations of this material. Nonetheless, the simulated values underestimated the measured concentrations by ~20%, and that was probably due to the effects of local meteorological conditions and uncertainties in the EC emission database for Hainan. The spatial distributions of horizontal winds at 200 m above the ground for the episode and the days before and after are shown in Fig. 6a. The prevailing winds over South China and the South China Sea were northeasterly on 30 January (first day) and 31 January (episode day). The simulated EC concentration on the first day was lower than the episode day in upstream areas and the PRD region was downwind. On 1 February, the day after the event, the simulated EC

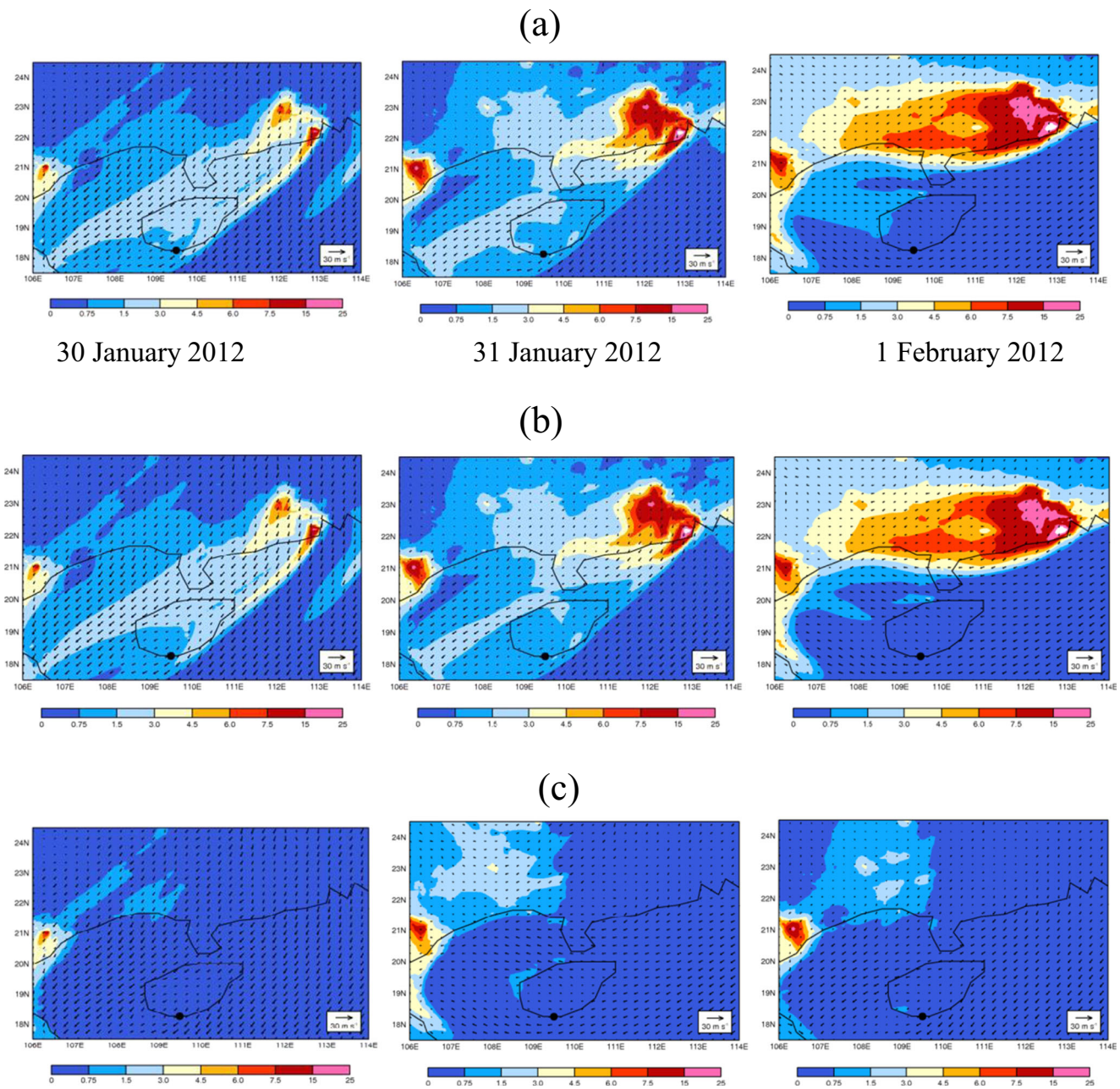

Fig. 6 Horizontal winds 200 m above ground level and **a** EC concentrations obtained with the Weather Research and Forecasting-Elemental or Black Carbon model at Hainan and surrounding areas and the EC model concentrations assuming **b** no emissions from Hainan and **c** no emissions from South China for 30 January to 1 February 2012

concentration in Sanya was the highest, but the winds to Sanya on that day came from east and passed over the South China Sea, which would have added little to the EC aerosol. As a result, higher concentrations of cluster 1 pollutants were measured in Sanya on the second day of the case study compared to those on the third day. More important, the model-based analysis indicates that emissions from Southern China, especially from the PRD region, were as the main source for the EC and other pollutants during the episode.

The contributions of local and regional emission to the pollution aerosol at Sanya also were estimated with the use of the WRF-BC model. Figure 6b, c depicts the simulated EC concentrations without emissions from Hainan and South China, respectively, during the pollution episode. The contribution of local primary emissions was only 18.1% of the total EC whereas emissions from areas to northeast of Sanya accounted for 76.8% of EC during the episode totally explained ca. 95% of the at least aerosol pollution origin

indicating that the main source during this episode is the primary emission pollutants from Hainan and South China.

Trace organic marker species, such as PAHs, can be used to evaluate regional impacts on air quality; indeed, vehicular emissions have been recognized as a common contributor to atmospheric pollution at both Sanya and the PRD region (Gao et al. 2012; Wang et al. 2015). Of the 3 days in the case study, the highest concentrations of benzo[a]pyrene (BaP), benzo[e]pyrene (BbP), and dibenzo[a,h]anthracene (DahA) were found on the day of the pollution episode. The PAHs most likely originated from industrial sources in the Guangdong Province in the PRD region (Wang et al. 2016), and benzo[k]fluoranthene (BfF), a marker for coal combustion (Ravindra et al. 2008), exhibited its highest concentration on 31 January (0.69 ng m^{-3}) compared with 0.21 and 0.42 ng m^{-3} on the other 2 days of the case study. In addition, the diagnostic ratio of indeno [1,2,3-cd]pyrene (IcdP)/(IcdP + benzo[ghi]perylene (BghiP)) was 0.52 on the episode day, and that was higher than the values < 0.50 on the first and third days of the case study. A combination of pollution emissions, such as those from wood fires, grass fires, and coal burning, is indicated for IcdP/(IcdP + BghiP) ratios > 0.5. Interestingly, the highest total quantified concentrations of PAHs and *n*-alkanes were found on the first day of the case study, not the episode day itself, and this demonstrates that the individual or diagnostic ratios of organic markers for specific source are useful for identification and tracking. The analysis of the case study provides further proof that transport from the PRD region can significantly impact the air quality at Sanya when the prevailing winds are from the northeast.

Conclusions

The chemical composition of $PM_{2.5}$ was measured and a mass balance of the $PM_{2.5}$ from Sanya was calculated to provide an overall assessment of the air quality during winter at the southernmost city on Hainan Island. The concentrations of typical pollutants were lower than in most Chinese cities due to geographical and climate conditions at Sanya and less industrial development. The low proportion of NH_4^+ in $PM_{2.5}$ suggested that the pollution sources were different from those in other areas and the main chemical reactions leading to SIA formation also were unlike those in some large cities. A thermodynamic model indicated that the aerosol acidities were relatively high and that acidity promoted heterogeneous reactions that led to aerosol SO_4^{2-}. Three major transport pathways were evaluated based on clusters of 3-day air-mass back trajectories. The air parcels that arrived at the site were predominately from the northeast, and the characteristics of the aerosol and pollution impacts varied among transport pathways. Transport from the South China, which was likely affected by emissions from the PRD region, brought polluted air to the site, and both regional influences and impacts from local emissions were evident. The WRF-EC model showed that regional emissions and transport was responsible for the high EC loadings, and the trajectories that passed over northeast Hainan province contributed 76.8% to the EC in $PM_{2.5}$. The evaluation based on trace organic markers supports the modeling results and demonstrates a close linkage between the pollutant loadings and transport from PRD region. One important implication of our finding is that maintaining or improving the air quality at clean sites such as Sanya will not only require effective controls on local emissions but also controls on distant sources. The results presented here were for a short sampling campaign, and more extensive measurements are needed to determine fully appreciate the relative influences of local emissions and atmospheric transport on air quality: a long-term study on the effects of the Asian monsoon and related large-scale processes would be particularly valuable. A more in-depth evaluation of the atmospheric reaction mechanisms between gases and particulate matter also should be performed with emphasis on their relations to air quality, regional environment, and climate.

Funding information This research is supported by the project from the "Strategic Priority Research Program" of the Chinese Academy of Science (Grant No. XDB05060500) and the project from Ministry of Science and Technology (2013FY112700). It is also supported by the Natural Science Foundation of Hainan Province, China (Grant No. 417151), The Doctoral Scientific Research Foundation of Hainan Tropical Ocean University (Grant No. RHDXB201613), Educational Reform of Hainan Tropical Ocean University (Grant No. RDJGb2016-18), and Key Discipline Construction Program of Hainan Provincial Department of Education (Marine Geology-2017).

References

Andreae MO, Barnard WR (1984) The marine chemistry of dimethylsulfide. Mar Chem 14(3):267–279. https://doi.org/10.1016/0304-4203(84)90047-1

Andrews E, Saxena P, Musarra S, Hildemann LM, Koutrakis P, McMurry PH, Olmez I, White WH (2011) Concentration and composition of atmospheric aerosols from the 1995 SEAVS experiment and a review of the closure between chemical and gravimetric measurements. J Air Waste Manage Assoc 50(5):648–664. https://doi.org/10.1080/10473289.2000.10464116

Battye W, Anejia VP, Roelle PA (2003) Evaluation and improvement of ammonia emissions inventories. Atmos Environ 37(27):3873–3883. https://doi.org/10.1016/S1352-2310(03)00343-1

Bencs L, Ravindra K, de HJ, Rasoazanany EO, Deutsch F, Bleux N, Berghmans P, Roekens E, Krata A, van Grieken R (2008) Mass and ionic composition of atmospheric fine particles over Belgium and their relation with gaseous air pollutants. J Environ Monit 10(10):1148–1157

Cao JJ, Lee SC, Ho KF, Zhang XY, Zou SC, Fung K, Chow JC, Watson JG (2003) Characteristics of carbonaceous aerosol in Pearl River Delta region, China during 2001 winter period. Atmos Environ 37(11):1451–1460. https://doi.org/10.1016/S1352-2310(02)01002-6

Cao JJ, Shen ZX, Chow JC, Watson JG, Lee SC, Tie XX, Ho KF, Wang GH, Han YM (2012) Winter and summer $PM_{2.5}$ chemical compositions in fourteen Chinese cities. J Air Waste Manag Assoc 62(10): 1214–1226. https://doi.org/10.1080/10962247.2012.701193

Cao J-J, Zhu C-S, Tie X-X, Geng F-H, Xu H-M, Ho SSH, Wang G-H, Han Y-M, Ho K-F (2013) Characteristics and sources of carbonaceous aerosols from Shanghai, China. Atmos Chem Phys 13(2): 803–817. https://doi.org/10.5194/acp-13-803-2013

Chandler AS, Choularton TW, Dollard GJ, Eggleton AEJ, Gay MJ, Hill TA, Jones BMR, Tyler BJ, Bandy BJ, Penkett SA (1988) Measurements of H_2O_2 and SO_2 in clouds and estimates of their reaction rate. Nature 336(6199):562–565. https://doi.org/10.1038/336562a0

Chen X, Yu JZ (2007) Measurement of organic mass to organic carbon ratio in ambient aerosol samples using a gravimetric technique in combination with chemical analysis. Atmos Environ 41(39):8857–8864. https://doi.org/10.1016/j.atmosenv.2007.08.023

Chow JC, Watson JG (1999) Ion chromatography in elemental analysis of airborne particles. In: Landsberger S, Creatchman M (eds) Elemental analysis of airborne particles. Gordon and Breach Science, Amsterdam, vol 1, pp 97–137

Chow JC, Watson JG, Pritchett LC, Pierson WR, Frazier CA, Purcell RG (1993) The dri thermal/optical reflectance carbon analysis system. Description, evaluation and applications in U.S. air quality studies. Atmos Environ Part A Gen Top 27(8):1185–1201. https://doi.org/10.1016/0960-1686(93)90245-T

Chow JC, Watson JG, Chen LWA, Arnott WP, Moosmüller H, Fung K (2004) Equivalence of elemental carbon by thermal/optical reflectance and transmittance with different temperature protocols. Environ Sci Technol 38(16):4414–4422

Chow JC, Yu JZ, Watson JG, Ho SSH, Bohannan TL, Hays MD, Fung KK (2007) The application of thermal methods for determining chemical composition of carbonaceous aerosols: a review. J Environ Sci Health A Tox Hazard Subst Environ Eng 42(11): 1521–1541. https://doi.org/10.1080/10934520701513365

Clegg SL, Brimblecombe P, Wexler AS (1998) Thermodynamic model of the system H^+–NH_4^+–SO_4^{2-} –NO_3^-–H_2O at tropospheric temperatures. J Phys Chem A 102(12):2137–2154. https://doi.org/10.1021/jp973042r

Cui S, Shi Y, Groffman PM, Schlesinger WH, Zhu Y-G (2013) Centennial-scale analysis of the creation and fate of reactive nitrogen in China (1910-2010). Proc Natl Acad Sci U S A 110(6):2052–2057. https://doi.org/10.1073/pnas.1221638110

Das M, Aneja VP (1994) Measurements and analysis of concentrations of gaseous hydrogen peroxide and related species in the rural Central Piedmont region of North Carolina. Atmos Environ 28(15):2473–2483. https://doi.org/10.1016/1352-2310(94)90398-0

El-Zanan HS, Lowenthal DH, Zielinska B, Chow JC, Kumar N (2005) Determination of the organic aerosol mass to organic carbon ratio in IMPROVE samples. Chemosphere 60(4):485–496. https://doi.org/10.1016/j.chemosphere.2005.01.005

El-Zanan HS, Zielinska B, Mazzoleni LR, Hansen DA (2012) Analytical determination of the aerosol organic mass-to-organic carbon ratio. J Air Waste Manag Assoc 59(1):58–69. https://doi.org/10.3155/1047-3289.59.1.58

Engelhart GJ, Hildebrandt L, Kostenidou E, Mihalopoulos N, Donahue NM, Pandis SN (2011) Water content of aged aerosol. Atmos Chem Phys 11(3):911–920. https://doi.org/10.5194/acp-11-911-2011

Feng J, Hu J, Xu B, Hu X, Sun P, Han W, Gu Z, Yu X, Wu M (2015) Characteristics and seasonal variation of organic matter in PM2.5 at a regional background site of the Yangtze River Delta region, China. Atmos Environ 123:288–297. https://doi.org/10.1016/j.atmosenv.2015.08.019

Friese E, Ebel A (2010) Temperature dependent thermodynamic model of the system H^+-NH_4^+-Na^+-SO_4^{2-}-NO_3^--Cl^--H_2O. J Phys Chem A 114(43):11595–11631. https://doi.org/10.1021/jp101041j

Fu X, Guo H, Wang X, Ding X, He Q, Liu T, Zhang Z (2015) $PM_{2.5}$ acidity at a background site in the Pearl River Delta region in fall-winter of 2007-2012. J Hazard Mater 286:484–492. https://doi.org/10.1016/j.jhazmat.2015.01.022

Fung CS, Misra PK, Bloxam R, Wong S (1991) A numerical experiment on the relative importance of H_2O_2, O_3 in aqueous conversion of SO2 to SO42-. Atmos Environ Part A Gen Top 25(2):411–423. https://doi.org/10.1016/0960-1686(91)90312-U

Gao B, Guo H, Wang X-M, Zhao X-Y, Ling Z-H, Zhang Z, Liu T-Y (2012) Polycyclic aromatic hydrocarbons in $PM_{2.5}$ in Guangzhou, southern China: spatiotemporal patterns and emission sources. J Hazard Mater 239-240:78–87. https://doi.org/10.1016/j.jhazmat.2012.07.068

Gu B, Sutton MA, Chang SX, Ge Y, Chang J (2014) Agricultural ammonia emissions contribute to China's urban air pollution. Front Ecol Environ 12(5):265–266. https://doi.org/10.1890/14.WB.007

Guan D, Su X, Zhang Q, Peters GP, Liu Z, Lei Y, He K (2014) The socioeconomic drivers of China's primary PM 2.5 emissions. Environ Res Lett 9(2):24010. https://doi.org/10.1088/1748-9326/9/2/024010

Guo S, Hu M, Zamora ML, Peng J, Shang D, Zheng J, Du Z, Wu Z, Shao M, Zeng L, Molina MJ, Zhang R (2014) Elucidating severe urban haze formation in China. Proc Natl Acad Sci U S A 111(49):17373–17378. https://doi.org/10.1073/pnas.1419604111

Guo J, Xia F, Zhang Y, Liu H, Li J, Lou M, He J, Yan Y, Wang F, Min M, Zhai P (2017) Impact of diurnal variability and meteorological factors on the PM2.5-AOD relationship. Implications for PM2.5 remote sensing. Environ Pollut 221:94–104. https://doi.org/10.1016/j.envpol.2016.11.043

He SZ, Chen ZM, Zhang X, Zhao Y, Huang DM, Zhao JN, Zhu T, Hu M, Zeng LM (2010) Measurement of atmospheric hydrogen peroxide and organic peroxides in Beijing before and during the 2008 Olympic Games. Chemical and physical factors influencing their concentrations. J Geophys Res 115(D17):459. https://doi.org/10.1029/2009JD013544

Ho SSH, Yu JZ (2004) In-injection port thermal desorption and subsequent gas chromatography-mass spectrometric analysis of polycyclic aromatic hydrocarbons and n-alkanes in atmospheric aerosol samples. J Chromatogr A 1059(1–2):121–129

Ho SSH, Yu JZ, Chow JC, Zielinska B, Watson JG, Sit EHL, Schauer JJ (2008) Evaluation of an in-injection port thermal desorption-gas chromatography/mass spectrometry method for analysis of non-polar organic compounds in ambient aerosol samples. J Chromatogr A 1200(2):217–227. https://doi.org/10.1016/j.chroma.2008.05.056

Ho SSH, Chow JC, Watson JG, Ting Ng LP, Kwok Y, Ho KF, Cao J (2011) Precautions for in-injection port thermal desorption-gas chromatography/mass spectrometry (TD-GC/MS) as applied to aerosol filter samples. Atmos Environ 45(7):1491–1496. https://doi.org/10.1016/j.atmosenv.2010.12.038

Hong YM, Lee BK, Park KJ, Kang MH, Jung YR, Lee DS, Kim MG (2002) Atmospheric nitrogen and sulfur containing compounds for three sites of South Korea. Atmos Environ 36(21):3485–3494. https://doi.org/10.1016/S1352-2310(02)00289-3

IPCC (2013) Climate Change 2013: the physical science basis. Contribution of working group I to the fifth assessment report of the intergovernmental panel on climate change. Cambridge University Press, Cambridge. https://doi.org/10.1017/CBO9781107415324

Keene WC, Pszenny APP, Galloway JN, Hawley ME (1986) Seasalt corrections and interpretation of constituent ratios in marine precipitation. J Geophys Res 91:6647–6658

Li L, Wang W, Feng J, Zhang D, Li H, Gu Z, Wang B, Sheng G, Fu J (2010) Composition, source, mass closure of PM2.5 aerosols for four forests in eastern China. J Environ Sci 22(3):405–412. https://doi.org/10.1016/S1001-0742(09)60122-4

Li XB, Huang H, Lian JS, Liu S, Huang LM, Yang JH (2013) Spatial and temporal variations in sediment accumulation and their impacts on coral communities in the Sanya Coral Reef Reserve, Hainan, China. Deep Sea Res Pt II 96:88–96. https://doi.org/10.1016/j.dsr2.2013.04.015

Li L, Yin Y, Kong S, Wen B, Chen K, Yuan L, Li Q (2014) Altitudinal effect to the size distribution of water soluble inorganic ions in PM at Huangshan, China. Atmos Environ 98:242–252. https://doi.org/10.1016/j.atmosenv.2014.08.077

Lippmann M, Xiong JQ, Li W (2000) Development of a continuous monitoring system for PM_{10} and components of $PM_{2.5}$. Appl Occup Environ Hyg 15(1):57–67. https://doi.org/10.1080/104732200301854

Liu D, Li J, Zhang Y, Xu Y, Liu X, Ding P, Shen C, Chen Y, Tian C, Zhang G (2013) The use of levoglucosan and radiocarbon for source apportionment of PM(2.5) carbonaceous aerosols at a background site in East China. Environ Sci Technol 47(18):10454–10461. https://doi.org/10.1021/es401250k

Meagher JF, Olszyna KJ, Weatherford FP, Mohnen VA (1990) The availability of H_2O_2 and O_3 for aqueous phase oxidation of SO_2. The question of linearity. Atmos Environ Part A Gen Top 24(7):1825–1829. https://doi.org/10.1016/0960-1686(90)90514-N

Meier PC, Zünd RE (2005) Statistical methods in analytical chemistry, 2nd edn. Chemical analysis, vol 153. Wiley, New York

Nguyen BC, Mihalopoulos N, Putaud JP, Gaudry A, Gallet L, Keene WC, Galloway JN (1992) Covariations in oceanic dimethyl sulfide, its oxidation products and rain acidity at Amsterdam Island in the southern Indian Ocean. J Atmos Chem 15(1):39–53. https://doi.org/10.1007/BF00053608

Niu Z, Zhang F, Chen J, Yin L, Wang S, Xu L (2013) Carbonaceous species in PM2.5 in the coastal urban agglomeration in the Western Taiwan Strait region, China. Atmos Res 122:102–110. https://doi.org/10.1016/j.atmosres.2012.11.002

Ohta S, Okita T (1990) A chemical characterization of atmospheric aerosol in Sapporo. Atmos Environ Part A Gen Top 24(4):815–822. https://doi.org/10.1016/0960-1686(90)90282-R

Pathak RK, Louie PKK, Chan CK (2004) Characteristics of aerosol acidity in Hong Kong. Atmos Environ 38(19):2965–2974. https://doi.org/10.1016/j.atmosenv.2004.02.044

Pathak RK, Wu WS, Wang T (2009) Summertime $PM_{2.5}$ ionic species in four major cities of China. Nitrate formation in an ammonia-deficient atmosphere. Atmos Chem Phys 9(5):1711–1722. https://doi.org/10.5194/acp-9-1711-2009

Pathak RK, Wang T, Ho KF, Lee SC (2011) Characteristics of summertime $PM_{2.5}$ organic and elemental carbon in four major Chinese cities. Implications of high acidity for water-soluble organic carbon (WSOC). Atmos Environ 45(2):318–325. https://doi.org/10.1016/j.atmosenv.2010.10.021

Pierson WR, Brachaczek WW (1983) Emissions of ammonia and amines from vehicles on the road. Environ Sci Technol 17(12):757–760. https://doi.org/10.1021/es00118a013

Pu W, Zhao X, Shi X, Ma Z, Zhang X, Yu B (2015) Impact of long-range transport on aerosol properties at a regional background station in Northern China. Atmos Res 153:489–499. https://doi.org/10.1016/j.atmosres.2014.10.010

Qiao YT, Zhang CH, Jian MQ (2015) Role of the 10–20-Day Oscillation in sustanined rainstorms over Hainan, China in October 2010. Adv Atmos Sci 32(3):363–374

Ravindra K, Sokhi R, Grieken RV (2008) Atmospheric polycyclic aromatic hydrocarbons: source attribution, emission factors and regulation. Atmos Environ 42(13):2895–2921

Seinfeld JH, Pandis SN (2006) Atmospheric Chemistry and Physics: from air pollution to climate change, 2nd edition. J Wiley, New York

Shen Z, Cao J, Arimoto R, Han Z, Zhang R, Han Y, Liu S, Okuda T, Nakao S, Tanaka S (2009a) Ionic composition of TSP and $PM_{2.5}$ during dust storms and air pollution episodes at Xi'an, China. Atmos Environ 43(18):2911–2918. https://doi.org/10.1016/j.atmosenv.2009.03.005

Shen ZX, Cao JJ, Tong Z, Liu SX, Reddy LSS, Han Y, Zhang T, Zhou J (2009b) Chemical characteristics of submicron particles in winter in Xi'an. Aerosol Air Qual Res:80–93. https://doi.org/10.4209/aaqr.2008.10.0050

Squizzato S, Masiol M, Brunelli A, Pistollato S, Tarabotti E, Rampazzo G, Pavoni B (2013) Factors determining the formation of secondary inorganic aerosol. A case study in the Po Valley (Italy). Atmos Chem Phys 13(4):1927–1939. https://doi.org/10.5194/acp-13-1927-2013

Stein AF, Draxler RR, Rolph GD, Stunder BJB, Cohen MD, Ngan F (2015) NOAA's HYSPLIT atmospheric transport and dispersion modeling system. Bull Am Meteorol Soc 96(12):2059–2077. https://doi.org/10.1175/BAMS-D-14-00110.1

Streets DG, Bond TC, Carmichael GR, Fernandes SD, Fu Q, He D, Klimont Z, Nelson SM, Tsai NY, Wang MQ, Woo J-H, Yarber KF (2003) An inventory of gaseous and primary aerosol emissions in Asia in the year 2000. J Geophys Res 108(D21):213. https://doi.org/10.1029/2002JD003093

Sutton MA, Dragosits U, Tang YS, Fowler D (2000) Ammonia emissions from non-agricultural sources in the UK. Atmos Environ 34(6):855–869. https://doi.org/10.1016/S1352-2310(99)00362-3

Sutton MA, Erisman JW, Dentener F, Möller D (2008) Ammonia in the environment: from ancient times to the present. Environ Pollut 156(3):583–604. https://doi.org/10.1016/j.envpol.2008.03.013

Thurston GD, Spengler JD (1985) A quantitative assessment of source contributions to inhalable particulate matter pollution in metropolitan Boston. Atmos Environ (1967) 19(1):9–25. https://doi.org/10.1016/0004-6981(85)90132-5

Walker JT, Whitall DR, Robarge W, Paerl HW (2004) Ambient ammonia and ammonium aerosol across a region of variable ammonia emission density. Atmos Environ 38(9):1235–1246. https://doi.org/10.1016/j.atmosenv.2003.11.027

Wang JZ, Ho SSH, Cao JJ, Huang RJ, Zhou JM, Zhao YZ, Xu HM, Liu SX, Wang GH, Shen ZX, Han YM (2015) Characteristics and major sources of carbonaceous aerosols in $PM_{2.5}$ from Sanya, China. Sci Total Environ 530-531:110–119. https://doi.org/10.1016/j.scitotenv.2015.05.005

Wang J, Ho SSH, Ma S, Cao J, Dai W, Liu S, Shen Z, Huang R, Wang G, Han Y (2016) Characterization of $PM_{2.5}$ in Guangzhou, China: uses of organic markers for supporting source apportionment. Sci Total Environ 550:961–971. https://doi.org/10.1016/j.scitotenv.2016.01.138

Watson JG (2002) Visibility: science and regulation. J Air Waste Manag Assoc 52(6):628–713

Watson JG, Chow JC, Frazier CA (1999) X-ray fluorescence analysis of ambient air samples. In: Landsberger S, Creatchman M (eds) Elemental analysis of airborne particles. Gordon and Breach Science, Amsterdam, vol 1, pp 67–96

Wilson LJ, Bacon PJ, Bull J, Dragosits U, Blackall TD, Dunn TE, Hamer KC, Sutton MA, Wanless S (2004) Modelling the spatial distribution of ammonia emissions from seabirds in the UK. Environ Pollut 131(2):173–185. https://doi.org/10.1016/j.envpol.2004.02.008

Wu Y, Gu B, Erisman JW, Reis S, Fang Y, Lu X, Zhang X (2016) $PM_{2.5}$ pollution is substantially affected by ammonia emissions in China. Environ Pollut 218:86–94. https://doi.org/10.1016/j.envpol.2016.08.027

Wu X, Deng JJ, Chen JS, Hong YW, Xu LL, Yin LQ, Du WJ, Hong ZY, Dai NZ, Yuan C-S (2017) Characteristics of water-soluble inorganic components and acidity of $PM_{2.5}$ in a coastal city of China. Aerosol Air Qual Res 17(9):2152–2164. https://doi.org/10.4209/aaqr.2016.11.0513

Xu HM, Cao JJ, Ho KF, Ding H, Han YM, Wang GH, Chow JC, Watson JG, Khol SD, Qiang J, Li WT (2012) Lead concentrations in fine particulate matter after the phasing out of leaded gasoline in Xi'an,

China. Atmos Environ 46:217–224. https://doi.org/10.1016/j.atmosenv.2011.09.078

Xu L, Yu Y, Yu J, Chen J, Niu Z, Yin L, Zhang F, Liao X, Chen Y (2013) Spatial distribution and sources identification of elements in PM2.5 among the coastal city group in the Western Taiwan Strait region, China. Sci Total Environ 442:77–85. https://doi.org/10.1016/j.scitotenv.2012.10.045

Xu H, Cao J, Chow JC, Huang R-J, Shen Z, Chen LWA, Ho KF, Watson JG (2016) Inter-annual variability of wintertime $PM_{2.5}$ chemical composition in Xi'an, China: evidences of changing source emissions. Sci Total Environ 545-546:546–555. https://doi.org/10.1016/j.scitotenv.2015.12.070

Yang G-P, Zhang H-H, Zhou L-M, Yang J (2011) Temporal and spatial variations of dimethylsulfide (DMS) and dimethylsulfoniopropionate (DMSP) in the East China Sea and the Yellow Sea. Cont Shelf Res 31(13):1325–1335. https://doi.org/10.1016/j.csr.2011.05.001

Yin L, Niu Z, Chen X, Chen J, Zhang F, Xu L (2014) Characteristics of water-soluble inorganic ions in PM2.5 and PM 2.5-10 in the coastal urban agglomeration along the Western Taiwan Strait region, China. Environ Sci Pollut Res Int 21(7):5141–5156. https://doi.org/10.1007/s11356-013-2134-7

Zhang Y, Seigneur C, Seinfeld JH, Jacobson M, Clegg SL, Binkowski FS (2000) A comparative review of inorganic aerosol thermodynamic equilibrium modules. Similarities, differences, and their likely causes. Atmos Environ 34(1):117–137. https://doi.org/10.1016/S1352-2310(99)00236-8

Zhang XY, Gong SL, Shen ZX, Mei FM, Xi XX, Liu LC, Zhou ZJ, Wang D, Wang YQ, Cheng Y (2003) Characterization of soil dust aerosol in China and its transport and distribution during 2001 ACE-Asia. 1. Network observations. J Geophys Res 108(D9). https://doi.org/10.1029/2002JD002632

Zhang Q, Jimenez JL, Worsnop DR, Canagaratna M (2007) A case study of urban particle acidity and its influence on secondary organic aerosol. Environ Sci Technol 41(9):3213–3219. https://doi.org/10.1021/es061812j

Zhang T, Cao JJ, Tie XX, Shen ZX, Liu SX, Ding H, Han YM, Wang GH, Ho KF, Qiang J, Li WT (2011) Water-soluble ions in atmospheric aerosols measured in Xi'an, China. Seasonal variations and sources. Atmos Res 102(1–2):110–119. https://doi.org/10.1016/j.atmosres.2011.06.014

Zhang X, Wu L, Zhang R, Deng S, Zhang Y, Wu J, Li Y, Lin L, Li L, Wang Y, Wang L (2013) Evaluating the relationships among economic growth, energy consumption, air emissions and air environmental protection investment in China. Renew Sust Energ Rev 18:259–270. https://doi.org/10.1016/j.rser.2012.10.029

Zhao PS, Dong F, He D, Zhao XJ, Zhang XL, Zhang WZ, Yao Q, Liu HY (2013) Characteristics of concentrations and chemical compositions for $PM_{2.5}$ in the region of Beijing, Tianjin, and Hebei, China. Atmos Chem Phys 13(9):4631–4644. https://doi.org/10.5194/acp-13-4631-2013

Zhao M, Huang Z, Qiao T, Zhang Y, Xiu G, Yu J (2015a) Chemical characterization, the transport pathways and potential sources of PM2.5 in Shanghai. Seasonal variations. Atmos Res 158-159:66–78. https://doi.org/10.1016/j.atmosres.2015.02.003

Zhao S, Tie X, Cao J, Li N, Li G, Zhang Q, Zhu C, Long X, Li J, Feng T, Su X (2015b) Seasonal variation and four-year trend of black carbon in the Mid-west China. The analysis of the ambient measurement and WRF-Chem modeling. Atmos Environ 123:430–439. https://doi.org/10.1016/j.atmosenv.2015.05.008